

Idaho State University

Wildland Fire Risk Assessment of Cascades Ecoregion in California

Christina Appleby

GEOL 5503: Principles of GIS

Professor Bottenberg

December 14, 2022

Table of Contents

Abstract	2
1. Introduction.....	2
1.1 California and Wildland Fires	2
1.2 Study Area.....	3
2. Data and Methodology.....	4
2.1 Risk Assessment Factors.....	4
2.2 Data Sources and Preprocessing	6
2.3 Fire Risk Classification	8
2.4 Wildland Fire Risk Assessment	10
3. Results.....	11
4. Conclusion	12
References	15
Appendix A: Geodatabases.....	20
Appendix B: Fire Risk Factors Maps.....	21
Appendix C: Fire Risk Factors Classification Maps.....	26
Appendix D: Wild Fire Risk Assessment Maps	33

Abstract

Wildland fires can have devastating effects on both natural resources and the environment. The purpose of this study was to assess the wildland fire risk of the Cascades ecoregion in California. This study identified several factors that affect wildland fire risk, including land cover, vegetation moisture, topography (aspect, slope, and elevation), and proximity to roads and urban areas. Using a geographic information system, the factors were classified according to fire risk, and a weighted calculation was used to produce a wildland fire risk assessment (WFRA) map for the beginning of July 2021. The WFRA successfully identified at-risk areas; however, the level of risk was not as high as expected compared to fire perimeters from 2021. Identifying areas at risk for wildland fires can alert homeowners to create defensible space around their homes and provide forest managers with a focus for reducing fuel loads.

1. Introduction

1.1 California and Wildland Fires

In many of California's ecosystems, wildland fires are a natural and common occurrence (Newcomer et al., 2019). Wildlands can benefit from low-severity fires by cleaning the forest floor, providing habitat, killing diseases and insects that prey on trees, and providing the intense heat required for fire-dependent seed germination of certain plants (*Benefits of Fire*, n.d.). However, there are also many adverse effects of wildland fires, such as the release of contaminants from biomass and manmade materials, increased air pollution, water quality impacts, and landslides (Newcomer et al., 2019). Wildland fires also destroy homes, timber lands, and transportation and utilities infrastructure (Feo et al., 2020).

Since 1990, wildland fire activity in California has increased, including fire occurrence, total acres burned, average fire size, and burn severity (Feo et al., 2020). Climate change has extended the fire season into the fall months because of increased temperatures and decreased precipitation (Goss et al., 2020). The increase in wildland fire activity comes at a great cost. The estimated annual value of structure losses in California from 2009 – 2018 was nearly \$1 billion (Buechi et al., 2021).

1.2 Study Area

The Cascades ecoregion encompasses much of the Cascades Mountain range and begins in central western Washington, through Oregon, and extends into northern California (Griffith et al., 2016). The northern California section of the Cascades ecoregion was chosen for the study area, which is part of the southern Cascades (Figure 1).

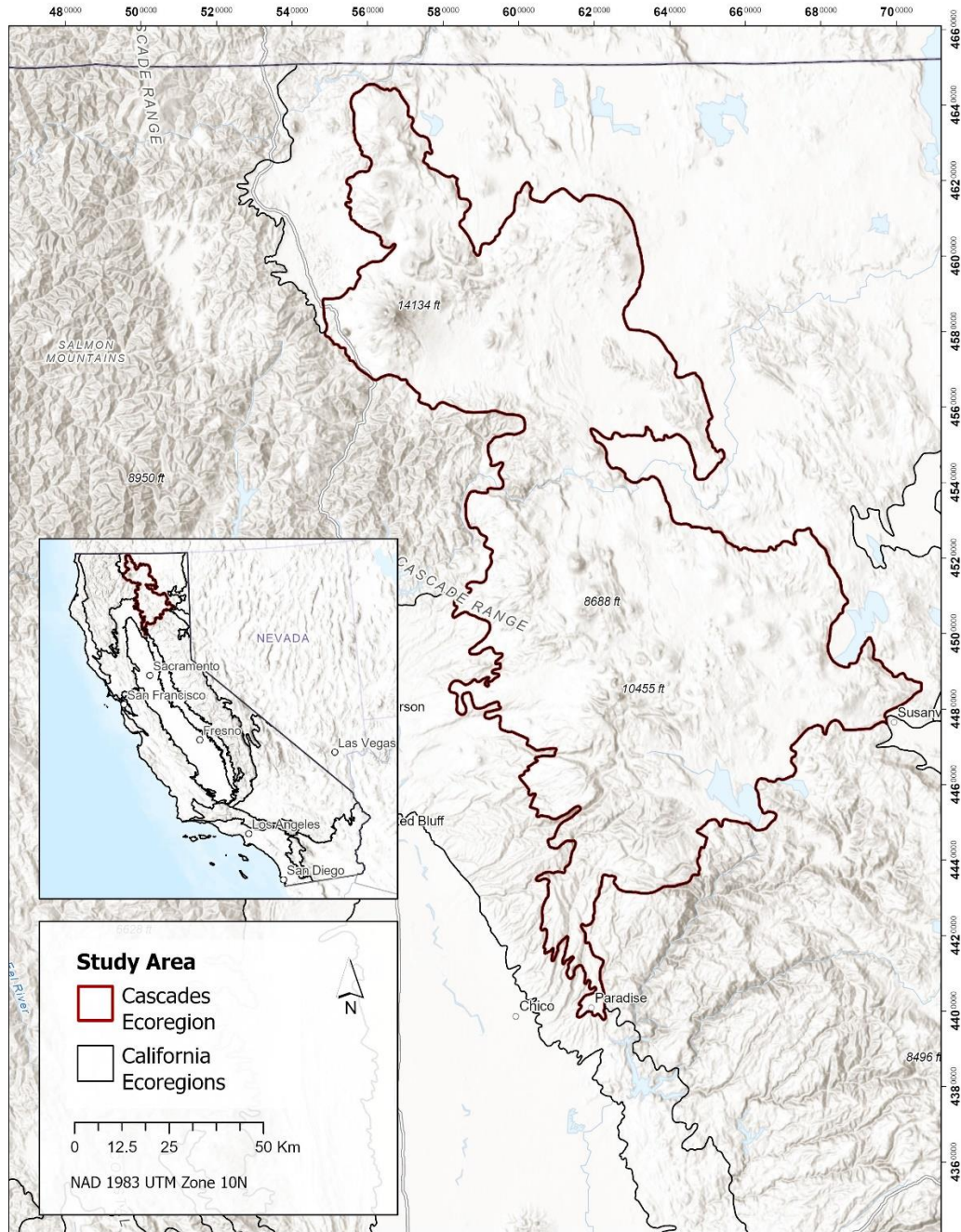


Figure 1 - Map of the Cascades ecoregion of California, the study area for this assessment.

The study area includes notable topographic features: Mount Shasta, Mount Lassen, Burney Falls, Hat Creek Valley, Pit River Canyon, and the Medicine Lake Highlands (Skinner & Taylor, 2018). A diverse mix of conifers dominates the landscape of the study area, such as ponderosa pines, lodgepole pines, white fir, red fir, and Douglas fir. Forty percent of California's surface water runoff flows from the Cascades and Sierra Nevada. The springs and creeks of the southern Cascades support many unique fish species (Griffith et al., 2016). Runoff after high-intensity wildland fires contains ash and debris that flows into and damages water sources (Snow, 2022).

The Cascades ecoregion has a mediterranean climate characterized by cool, wet winters and warm, dry summers. Lightning strikes are a common wildland fire ignition source, and lightning is common throughout the Cascades Mountain range. Specific but infrequent weather patterns can cause widespread thunderstorms that ignite hundreds of wildland fires in a short period of time (Skinner & Taylor, 2018).

2. Data and Methodology

All data were processed and analyzed using ArcGIS Pro and Microsoft Excel. Figures of geodatabases used for data processing and analysis can be found in Appendix A. Maps of the different risk assessment factors can be found in Appendix B.

2.1 Risk Assessment Factors

Fuel

Land cover is fuel for wildland fires. Fuel models have been used by the United States Department of Agriculture since the 1960s to predict fire danger indices and potential fire behavior (Anderson, 1982). Different types of land cover are more prone to fire (Barros & Pereira, 2014), making it a key factor in this assessment.

Fuel moisture content, whether from live or dead fuels, is another key factor in ignition and propagation (*Weather and Fuel Moisture / NWCG*, n.d.). Drought affects the fuel moisture of live and dead fuels, making them more flammable and ignition more probable (Littell et al., 2016). Two popular spectral indices for assessing drought are the Normalized Difference Vegetation Index (NDVI) and Normalized Difference Moisture Index (NDMI). NDVI quantifies

green vegetation and NDMI quantifies vegetation water content. NDMI was chosen because it is more sensitive than NDVI and is used more often in assessing wildland fire potential (Parks et al., 2018). Additionally, NDMI has a stronger correlation to land surface temperature than NDVI (Li et al., 2017), and increases land surface temperature increase the likelihood of wildland fires (Yang, 2021).

The land cover of the study area is primarily conifer and shrubland. Conifers retain their foliage longer, and older foliage has a low moisture content. This is one of the reasons conifer live foliage is more combustible than hardwood live foliage (*Weather and Fuel Moisture / NWCG*, n.d.), making conifers more susceptible to fire.

Topography

Land cover and fuel moisture are variable factors that affect wildland fire risk, whereas topography is stable. Topographic variables in wildland fire risk include slope, aspect, and elevation. Steeper slopes allow for more preheating of fuels upslope of a fire, resulting in the fire spreading faster (*Topographic Influences on Wildland Fire Behavior: Print Version*, n.d.).

Elevation affects fuel drying during fire season. Fuels at lower elevations tend to dry out earlier in the season, and fuels at higher elevations take longer to dry out. Lightning strikes are more frequent at higher elevations (Bennett et al., 2010), which caused 32% of wildland fires (greater than 300 acres) in California from 2001 – 2020 (*Fire Perimeters*, 2022).

Aspect affects levels of solar radiation, which affects fuel temperature. It also affects vegetation type and fuel loading (Bennett et al., 2010). South and southwest aspects receive higher solar radiation and have higher fuel temperatures and drier fuels (*Topographic Influences on Wildland Fire Behavior: Print Version*, n.d.), but they also have less vegetation and less fuel loading (Bennett et al., 2010). North aspects receive less solar radiation and are cooler with higher humidity (*Topographic Influences on Wildland Fire Behavior: Print Version*, n.d.). Because of this, north aspects also have more vegetation and heavier fuel loading, which can affect fire severity (Bennett et al., 2010). However, fire severity is not analyzed in this assessment, so only the effects of aspect on fuel temperature and moisture were considered.

Proximity to Roads and Urban Areas

From 2017 – 2020, approximately 89 percent of wildland fires in the U.S. were caused by humans (*Wildfire Statistics*, 2022). The proximity to roads and urban areas are two of the most important factors involving human-caused wildland fires (Romero-Calcerrada et al., 2008). The transition area between wildland areas and human development is known as the wildland urban interface (WUI), which grew by 33 percent from 1990 – 2020 (*Wildland Urban Interface: A Look at Issues and Resolutions*, 2022). Growth of the WUI not only puts more homes, infrastructure, and communities at risk, it also increases human interaction with wildland areas. Approximately 61 percent of human-caused wildland fires in the contiguous U.S. from 1986 – 1996 occurred within 200 meters of the nearest road (Morrison, 2007), and there is also a strong correlation between distance to urban areas and fire ignition probability (Catry et al., 2009).

2.2 Data Sources and Preprocessing

The California ecoregions vector dataset was obtained from the U.S. Environmental Protection Agency Ecosystems Research website. The Cascades ecoregion was exported as the study area boundary.

Landsat 8 rasters were obtained from the U.S. Geological Survey (USGS) Earth Explorer. Three Landsat tiles were needed to cover the study area; two of the tiles were acquired on June 25, 2021, and one was acquired on July 2, 2021. Composite band rasters of each tile were imported, reprojected, and added to a mosaic dataset. The mosaic was then clipped to the study area. The NDMI was calculated using the near-infrared and short-wave infrared bands (Equation 1).

$$NDMI = (NIR - SWIR) / (NIR + SWIR)$$

Equation 1 - Normalized difference moisture index calculation.

Shuttle Radar Topography Mission data were also obtained from the USGS Earth Explorer for the DEM and were acquired already void-filled. The DEM rasters were added to a mosaic dataset, reprojected, and clipped to the study area. The DEM was used to create slope and aspect rasters.

The Existing Vegetation Type (EVT) raster dataset from 2020 obtained from LANDFIRE was used for land cover. The EVT raster was reprojected and clipped to the study area. The raster was then reclassified based on physiognomy. Low-, medium- and high-intensity developed and developed physiognomies were reclassified into one class to represent all urban areas (Figure 2).

Separate urban and road feature classes were created by converting the land cover raster to polygons and exporting the urban and road features. The multiple ring buffer tool was then used to create buffers around each feature class according to their respective fire risk classification (Table 3). A union was performed with the buffer feature classes and the study area to cover the entire study area and create complete datasets. Although a large portion of the urban area buffers overlaps the road buffers, each was kept as a separate fire risk factor.

Value	New
Open Water	7
Quarries-Strip Mines-Gravel Pits-	8
Developed-Low Intensity	9
Developed-Medium Intensity	9
Developed-High Intensity	9
Developed-Roads	12
Sparsely Vegetated	13
Snow-Ice	14
Developed	9
Agricultural	16
Exotic Herbaceous	17
Exotic Tree-Shrub	18

Figure 2 - Reclassification of developed areas for EVT raster.

The fire perimeters dataset was obtained from the California of Forestry and Fire Protection's (CAL FIRE) Fire and Resource Assessment Program. The vector dataset included fires from 1878 – 2021. The vector dataset was imported and reprojected. CAL FIRE classifies large fires as fires that are 300 acres or greater. To reduce the size of the dataset for us in risk classification, fire perimeters 300 acres or greater from 2001 – 2020 were exported into a feature class. The fire perimeters were then clipped to the study area. Fire perimeters from 2021, regardless of size, that intersected with the study area were also exported into a separate feature class for evaluating the WFRA.

The fire ignition point dataset (FireOccurrence) was obtained from the U.S. Forest Service (USFS) and represents ignition points for fires in USFS wildlands. First, points from 2021 were

exported into a feature class. The points were then clipped to the study area. Finally, fire ignition points of fires one acre or greater were exported into a feature class. These data were not used for the WFRA; they were used to evaluate the effectiveness of the assessment.

2.3 Fire Risk Classification

Each factor was classified on a scale of 1 to 5 with 1 as a very low fire risk and 5 as a very high fire risk. Fire risk classification maps can be found in Appendix C.

The fire risk classification for slope was determined using the reduced fire perimeters dataset. The slope raster was reclassified to intervals of 5 percent from 0 – 45 percent and a final interval of 45 – 90 percent. The reclassified slope raster was clipped to the fire perimeters. The pixel count field from the unclipped raster was joined to the clipped raster. The percentage of pixels in each slope interval was then calculated (Equation 2 and Table 1). This percentage was used for the risk classification (Table 3).

$$\% = \frac{\text{# of pixels in fire perimeter}}{\text{# of total pixels in the study area}}$$

Equation 2 - Calculation for the percentage of pixels in the fire perimeters.

Slope (percent)	%
0 – 5	6
5 – 10	7
10 – 15	9
15 – 20	10
20 – 25	11
25 – 30	13
30 – 35	15
35 – 40	17
40 – 45	18
> 45	15

Table 1 – Slope interval percentages.

The reduced fire perimeters dataset was also used for elevation fire risk classification. The Zonal Statistics as Table tool was used with the fire perimeters as the input feature zone using the OBJECTID as the zone field, and the DEM as the input value raster. The median elevation was calculated for each fire perimeter. The median elevation field from the zonal statistic table was joined with the fire perimeters attribute table. The natural break classification was obtained using the median field for symbology. The elevation fire risk classification was based on these values as well as research from Adab et al. (2012).

Land cover was classified based on research from Hanberry (2020) and Adaktylou et al. (2020). The NDMI was classified based on information from EOS Data Analytics (*Normalized Difference Moisture Index: Equation and Interpretation*, 2022). Proximity to urban areas was classified based on research from Adab et al. (2012) and González et al. (2006). Proximity to roads was based on research from Morrison (2007). Aspect was classified based on information on the National Wildfire Coordinating Group website (*Topographic Influences on Wildland Fire Behavior: Print Version*, n.d.). These classifications can be seen in Table 3.

Land Cover	Value
Water, Snow-Ice	0
Riparian, Quarries, Agricultural, Hardwood, Urban, Roads	1
Sparingly Vegetated	2
Tree-shrub	3
Shrubland, Conifer-Hardwood	4
Herbaceous, Grassland, Conifer	5

Table 2 - Land cover fire risk classification.

Value	NDMI	Aspect	Slope (%)	Elevation (m)	Urban (m)	Roads (m)
1	> 0.33	N, Flat	< 5	> 2000	> 2000	> 800
2	0.15 – 0.33	NE, NW	5 – 10	1600 – 2000	1500 – 2000	-
3	0.06 – 0.15	SE, E	10 – 15	1200 – 1600	1000 – 1500	400-800
4	0 – 0.06	W	15 – 20	1000 – 1200	500 – 1000	200 – 400
5	< 0	S, SW	> 20	< 1000	< 500	< 200

Table 3 – Fire risk classifications.

To assign fire risk classification values, each raster was reclassified according to Table 2 and Table 3. A fire risk classification field was added to the attribute table for the feature classes. Each feature class was then converted to a raster with the risk classification field as the raster value and cell size of 30. Maps of each factor's fire risk classification can be found in Appendix B.

2.4 Wildland Fire Risk Assessment

The WFRA was performed using the Weighted Sum Tool. A pairwise comparison was used to weigh each factor in the WFRA calculation (Table 4 and Table 5). Two assessments were performed with certain factors weighted differently based on research from Tien Bui et al. (2016) and Romero-Calcerrada et al. (2008).

	LC	NDMI	Aspect	Slope	Urban	Roads	Elevation
LC	LC						
NDMI	LC	M					
Aspect	LC	M	A				
Slope	LC	M	A	S			
Urban	LC	M	A	S	U		
Roads	LC	M	A	S	U	R	
Elevation	LC	M	A	S	U	R	E
Weight	0.25	0.21	0.18	0.14	0.11	0.07	0.04

Table 4 - WFRA 1 pairwise comparison and weighted values.

	LC	NDMI	Urban	Roads	Aspect	Slope	Elevation
LC	LC						
NDMI	LC	M					
Urban	LC	M	U				
Roads	LC	M	U	R			
Aspect	LC	M	U	R	A		
Slope	LC	M	U	R	A	S	
Elevation	LC	M	U	R	A	S	E
Weight	0.25	0.21	0.18	0.14	0.11	0.07	0.04

Table 5 - WFRA 2 pairwise comparison and weighted values.

3. Results

The results of WFRA 1 and WFRA 2 can be seen in Figure 3. The higher factor weights for proximity to urban and roads are clearly shown in WFRA 2. Overall, WFRA 1 shows more areas with a higher fire risk than WFRA 2 (Figure 4). Both assessments were evaluated using the fire perimeters from 2021. WFRA 1 had higher fire risk pixels in the fire perimeters than WFRA 2 (Figure 5). The assessments were also evaluated using the fire ignition points from 2021 for fires one acre or greater (Figure 6). For most fire ignition points, WFRA 1 had a higher fire risk than WFRA 2. Based on these evaluations, WFRA 1 more accurately assessed wildland fire risk than WFRA 2.

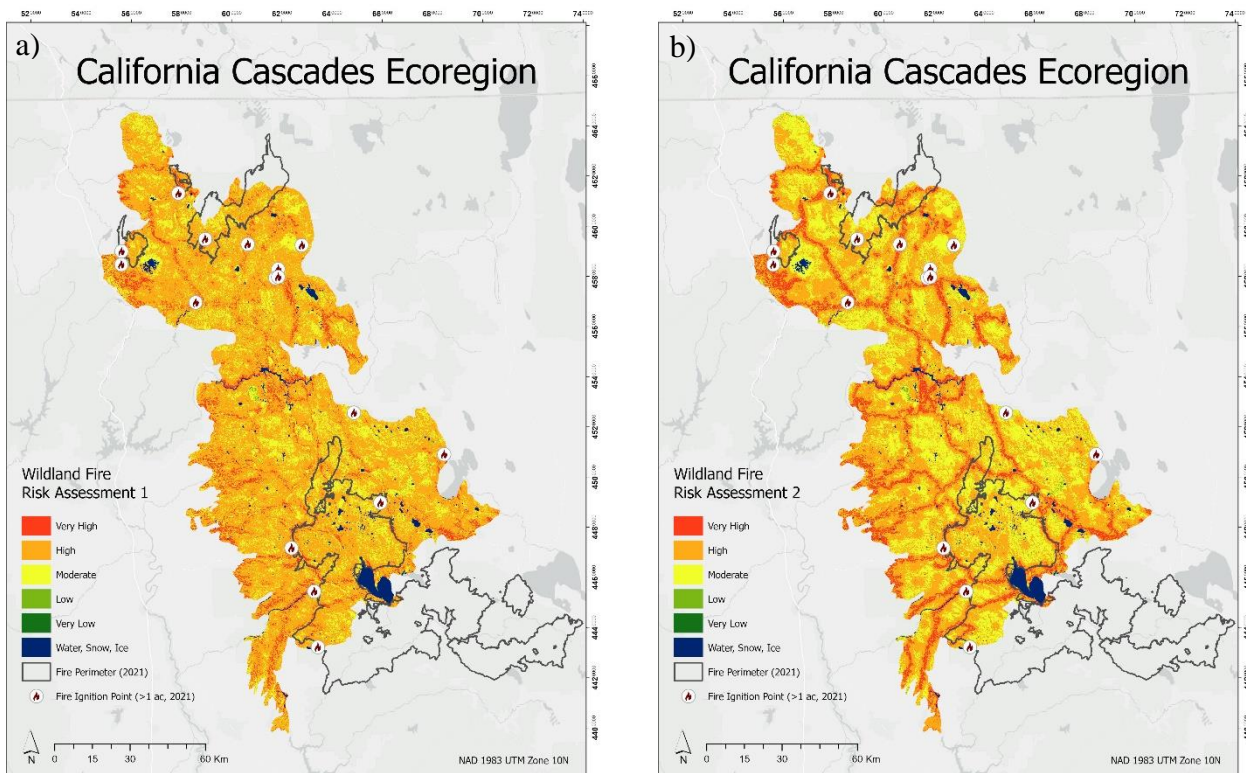


Figure 3 - WFRA 1 (a) and 2 (b) with fire perimeters from 2021 and fire ignition points for fires one acre or greater from 2021.

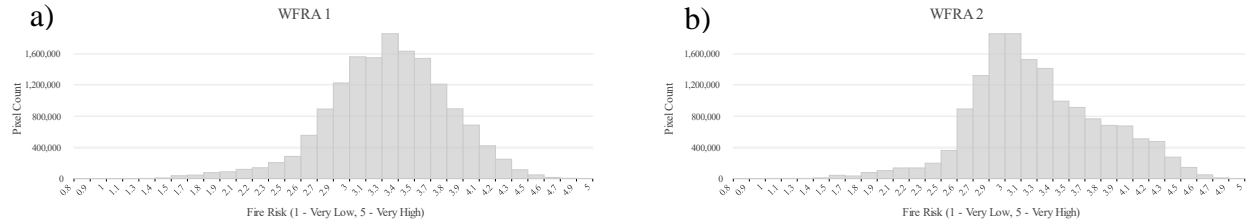


Figure 4 - Histogram of fire risk values and pixel count for study area for WFRA 1 (a) and 2 (b).

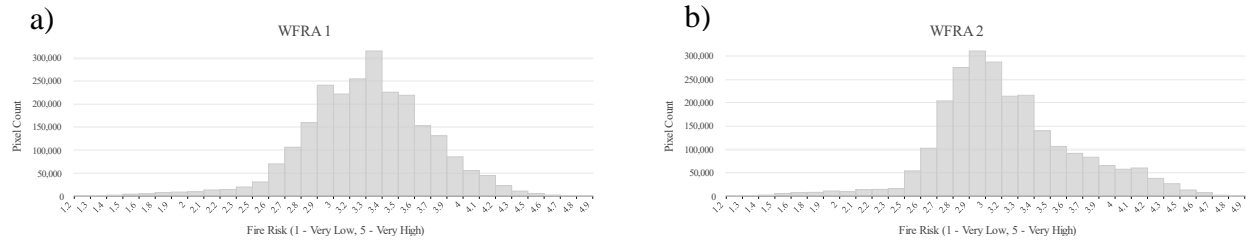


Figure 5 - Histogram of fire risk values and pixel count for fire perimeters from 2021 for WFRA 1 (a) and WFRA 2 (b)

WFRA 1	3.93	4.04	3.49	3.10	3.93	3.43	3.03	2.86	2.89	3.74	3.53	3.84	4.00	3.46	4.00	4.17
WFRA 2	4.07	3.83	3.14	3.03	4.07	3.15	2.89	2.72	2.82	3.60	3.18	3.42	4.00	3.25	4.42	3.75

Figure 6 - Fire risk values for fire perimeters one acre or greater from 2021 for WFRA 1 and 2.

4. Conclusion

The simplicity of this assessment provides a basic reference of areas at risk for wildland fires in the Cascades Ecoregion of California. However, there are ways this type of assessment could be improved.

The land cover for the study area was primarily conifer and shrubland (Table 6), which makes the land cover fire risk classification for 84 percent of the study area constant. Land cover was given the most weight in the WFRA calculation, and both conifer and shrubland land covers were classified with a fire risk value of 4. This could explain the lower fire risk values in the WFRAAs. Because of this, land cover could be given less weight in future WFRA calculations and

a more variable factor, such as NDMI, could be given more weight. Additionally, instead of using the LANDFIRE existing vegetation types for land cover, a land cover land use classification could be performed using Landsat imagery or another type of multispectral imagery.

Land Cover	Percent
Conifer	74.6
Shrubland	10.4
Riparian	3.7
Sparsely Vegetated	3.0
Hardwood	1.5
Roads	1.4
Open Water	1.2
Grassland	1.2
Exotic Herbaceous	1.1
Urban	1.1
Agricultural	0.7
Snow-Ice	0.05
Quarries, Gravel, etc.	0.04
Conifer-Hardwood	0.004
Exotic Tree-Shrub	0.0002

Table 6 - Percentage of land cover type for study area calculated using pixel counts.

The NDMI was calculated using Landsat data from June 25, 2021, and July 2, 2021. Ten of the fire ignition points and five of the fire perimeters used to evaluate the WFRA had a fire start date after the Landsat imagery acquisition. After the Landsat imagery acquisition date, the drought conditions in California worsened (Figure 7). As a result, NDMI calculations later in the fire season would likely have been lower, increasing the risk of fire in the study area.

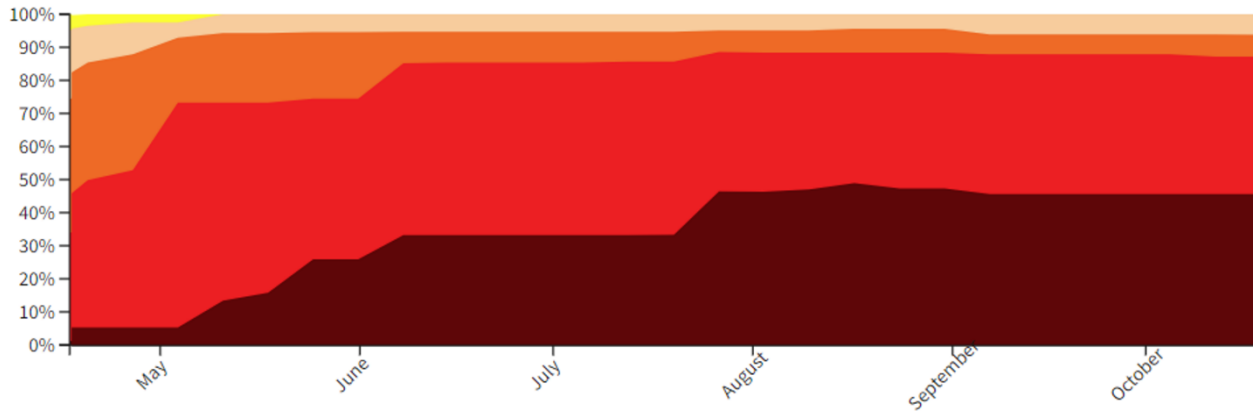


Figure 7 - Graph of Historical U.S. Drought Monitor for California from mid-April to mid-October 2021 from the National Integrated Drought Information System.

(D0 - Abnormally Dry, D1 - Moderate Drought, D2 - Severe Drought, D3 - Extreme Drought, D4 - Exceptional Drought)

More research could be done to determine more accurate elevation fire risk classifications. As the climate changes, wildland fires are burning at elevations once too high and too wet burn (Alizadeh et al., 2021). Out of 16 fire ignition points, only one had an elevation fire risk classification of greater than 3.

The proximity to urban areas and proximity to roads fire risk classifications overlapped each other significantly as many of the urban areas encompassed roads. In future WFRAs, these two factors could be more distinctly separated to prevent high overlap.

Other factors could also be included to improve the WFRA:

- Previously burned areas (Syphard et al., 2008)
- Areas of excessive fuel loading due to fire suppression (Keeley & Syphard, 2021)
- Atmospheric factors such as temperature, wind, and humidity (Gai et al., 2011)

Additionally, separate WFRAs could be performed for natural-caused and human-caused wildland fires. Moreover, creating a statistical model of wildland fire risk would greatly improve this assessment (Prestemon et al., 2013).

References

- Adab, H., Kanniah, K. D., & Solaimani, K. (2012). Modeling forest fire risk in the northeast of Iran using remote sensing and GIS techniques. *Natural Hazards*, 65(3), 1723–1743. <https://doi.org/10.1007/s11069-012-0450-8>
- Adaktylou, N., Stratoulias, D., & Landenberger, R. (2020). Wildfire Risk Assessment Based on Geospatial Open Data: Application on Chios, Greece. *ISPRS International Journal of Geo-Information*, 9(9), 516. <https://doi.org/10.3390/ijgi9090516>
- Alizadeh, M. R., Abatzoglou, J. T., Luce, C. H., Adamowski, J. F., Farid, A., & Sadegh, M. (2021). Warming enabled upslope advance in western US forest fires. *Proceedings of the National Academy of Sciences*, 118(22). <https://doi.org/10.1073/pnas.2009717118>
- Anderson, H. E. (1982). *Aids to Determining Fuel Models For Estimating Fire Behavior* (INT-122). U.S. Department of Agriculture, Forest Service. <https://www.fs.usda.gov/research/treesearch/6447>
- Barros, A. M. G., & Pereira, J. M. C. (2014). Wildfire Selectivity for Land Cover Type: Does Size Matter? *PLoS ONE*, 9(1), e84760. <https://doi.org/10.1371/journal.pone.0084760>
- Benefits of Fire*. (n.d.). California Department of Forestry and Fire Protection. Retrieved December 10, 2022, from <https://www.fire.ca.gov/media/5425/benifitsoffire.pdf>
- Bennett, M., Fitzgerald, S. A., Parker, R. T., Schnepf, C., Main, M., Perleberg, A., & Mahoney, R. (2010). *Reducing Fire Risk on Your Forestland Property* (PNW 618). Oregon State University Extension Service. <https://catalog.extension.oregonstate.edu/pnw618>
- Buechi, H., Weber, P., Heard, S., Cameron, D., & Plantinga, A. J. (2021). Long-term trends in wildfire damages in California. *International Journal of Wildland Fire*, 30(10), 757. <https://doi.org/10.1071/wf21024>
- California Department of Fish and Wildlife. (2015). *California State Wildlife Action Plan, Vol. 1, Ch. 5.2* (A. G. Gonzales & J. Hoshi, Eds.; SWAP 2015). <https://nrm.dfg.ca.gov/FileHandler.ashx?DocumentID=109208&inline>

- Catry, F. X., Rego, F. C., Baçao, F. L., & Moreira, F. (2009). Modeling and mapping wildfire ignition risk in Portugal. *International Journal of Wildland Fire*, 18(8), 921. <https://doi.org/10.1071/wf07123>
- Costa-Saura, J. M., Balaguer-Beser, N., Ruiz, L. A., Pardo-Pascual, J. E., & Soriano-Sancho, J. L. (2021). Empirical Models for Spatio-Temporal Live Fuel Moisture Content Estimation in Mixed Mediterranean Vegetation Areas Using Sentinel-2 Indices and Meteorological Data. *Remote Sensing*, 13(18), 3726. <https://doi.org/10.3390/rs13183726>
- Feo, T. J., Evans, S., Mace, A. J., Brady, S. E., & Lindsey, B. (2020). *The Costs of Wildfire in California* (No. 978-1-930117-66-2). California Council on Science and Technology. <https://ccst.us/reports/the-costs-of-wildfire-in-california/>
- Fire Perimeters*. (2022). [Dataset]. California Department of Forestry and Fire Protection's Fire Resource Assessment Program. <https://frap.fire.ca.gov/mapping/gis-data/>
- Gai, C., Weng, W., & Yuan, H. (2011). GIS-Based Forest Fire Risk Assessment and Mapping. *2011 Fourth International Joint Conference on Computational Sciences and Optimization*. <https://doi.org/10.1109/cso.2011.140>
- González, J. R., Palahí, M., Trasobares, A., & Pukkala, T. (2006). A fire probability model for forest stands in Catalonia (north-east Spain). *Annals of Forest Science*, 63(2), 169–176. <https://doi.org/10.1051/forest:2005109>
- Goss, M., Swain, D. L., Abatzoglou, J. T., Sarhadi, A., Kolden, C. A., Williams, A. P., & Diffenbaugh, N. S. (2020). Climate change is increasing the likelihood of extreme autumn wildfire conditions across California. *Environmental Research Letters*, 15(9), 094016. <https://doi.org/10.1088/1748-9326/ab83a7>
- Griffith, G. E., Omernik, J. M., Smith, D. W., Cook, T. D., Tallyn, E., Moseley, K., & Johnson, C. B. (2016). Ecoregions of California. *Open-File Report*. <https://doi.org/10.3133/ofr20161021>
- Hanberry, B. B. (2020). Classifying Large Wildfires in the United States by Land Cover. *Remote Sensing*, 12(18), 2966. <https://doi.org/10.3390/rs12182966>

- Keeley, J. E., & Syphard, A. D. (2021). Large California wildfires: 2020 fires in historical context. *Fire Ecology*, 17(1). <https://doi.org/10.1186/s42408-021-00110-7>
- Li, B., Wang, H., Qin, M., & Zhang, P. (2017). Comparative study on the correlations between NDVI, NDMI and LST. *Progress in Geography*, 36(5), 585–596. <https://doi.org/10.18306/dlkxjz.2017.05.006>
- Littell, J. S., Peterson, D. L., Riley, K. L., Liu, Y., & Luce, C. H. (2016). A review of the relationships between drought and forest fire in the United States. *Global Change Biology*, 22(7), 2353–2369. <https://doi.org/10.1111/gcb.13275>
- McEvoy, D., Hobbins, M., Brown, T., VanderMolen, K., Wall, T., Huntington, J., & Svoboda, M. (2019). Establishing Relationships between Drought Indices and Wildfire Danger Outputs: A Test Case for the California-Nevada Drought Early Warning System. *Climate*, 7(4), 52. <https://doi.org/10.3390/cli7040052>
- Morrison, P. H. (2007). *Roads and Wildfires*. Pacific Biodiversity Institute. <http://pacificbio.org/publications/wildfire.htm>
- Newcomer, M., Prunicki, M., & Webster, J. (2019). *Environmental Impacts of Wildfires in California* (S. Hubbard, Interviewer). California Council on Science & Technology. <https://ccst.us/wp-content/uploads/CCST-One-Pager-Wildfire-Enviromental-Impacts-4-4-2019.pdf>
- Normalized Difference Moisture Index: Equation And Interpretation*. (2022, July 27). EOS Data Analytics. <https://eos.com/make-an-analysis/ndmi/>
- Parks, S. A., Holsinger, L. M., Panunto, M. H., Jolly, W. M., Dobrowski, S. Z., & Dillon, G. K. (2018). High-severity fire: evaluating its key drivers and mapping its probability across western US forests. *Environmental Research Letters*, 13(4), 044037. <https://doi.org/10.1088/1748-9326/aab791>
- Prestemon, J. P., Hawbaker, T. J., Bowden, M., Carpenter, J., Brooks, M. T., Abt, K. L., Sutphen, R., & Scranton, S. (2013). Wildfire Ignitions: A Review of the Science and Recommendations for Empirical Modeling. *U. S. Department of Agriculture Forest Service General Technical Report*. <https://doi.org/10.2737/srs-gtr-171>

- Romero-Calcerrada, R., Novillo, C. J., Millington, J. D. A., & Gomez-Jimenez, I. (2008). GIS analysis of spatial patterns of human-caused wildfire ignition risk in the SW of Madrid (Central Spain). *Landscape Ecology*, 23(3), 341–354. <https://doi.org/10.1007/s10980-008-9190-2>
- Skinner, C. N., & Taylor, A. H. (2018). *Fire in California's Ecosystems, Ch. 10* (J. V. W. Wagtendonk, N. G. Sugihara, S. L. Stephens, A. E. Thode, K. E. Shaffer, J. A. Fites-Kaufman, & J. K. Agee, Eds.; Second Edition, Revised). University of California Press.
- Snow, M. (2022, October 11). *How Does Wildfire Impact Wildlife and Forests?* U.S. Fish & Wildlife Service. Retrieved December 10, 2022, from <https://www.fws.gov/story/2022-10/how-does-wildfire-impact-wildlife-and-forests>
- Syphard, A. D., Radeloff, V. C., Keuler, N. S., Taylor, R. S., Hawbaker, T. J., Stewart, S. I., & Clayton, M. K. (2008). Predicting spatial patterns of fire on a southern California landscape. *International Journal of Wildland Fire*, 17(5), 602. <https://doi.org/10.1071/wf07087>
- Tien Bui, D., Le, K. T., Nguyen, V., Le, H., & Revhaug, I. (2016). Tropical Forest Fire Susceptibility Mapping at the Cat Ba National Park Area, Hai Phong City, Vietnam, Using GIS-Based Kernel Logistic Regression. *Remote Sensing*, 8(4), 347. <https://doi.org/10.3390/rs8040347>
- Topographic Influences on Wildland Fire Behavior: Print Version.* (n.d.). <http://stream1.cmatc.cn/pub/comet/FireWeather/S290Unit2TopographicInfluencesonWildlandFireBehavior/comet/fire/s290/unit2/print.htm>
- Weather and Fuel Moisture / NWCG.* (n.d.). <https://www.nwcg.gov/publications/pms425-1/weather-and-fuel-moisture>
- Wildfire Statistics (IF 10244).* (2022). Congressional Research Service. <https://crsreports.congress.gov/>
- Wildland Urban Interface: A Look at Issues and Resolutions.* (2022). U.S. Fire Adminstration. <https://www.usfa.fema.gov/downloads/pdf/publications/wui-issues-resolutions-report.pdf>

Yang, S. (2021). *The Relationship between Land Surface Temperature Anomalies and Fire Occurrence in Cariboo Region in 2017* [Dataset]. University of British Columbia Library. <https://doi.org/10.5683/SP2/FVQ6VB>

Appendix A: Geodatabases

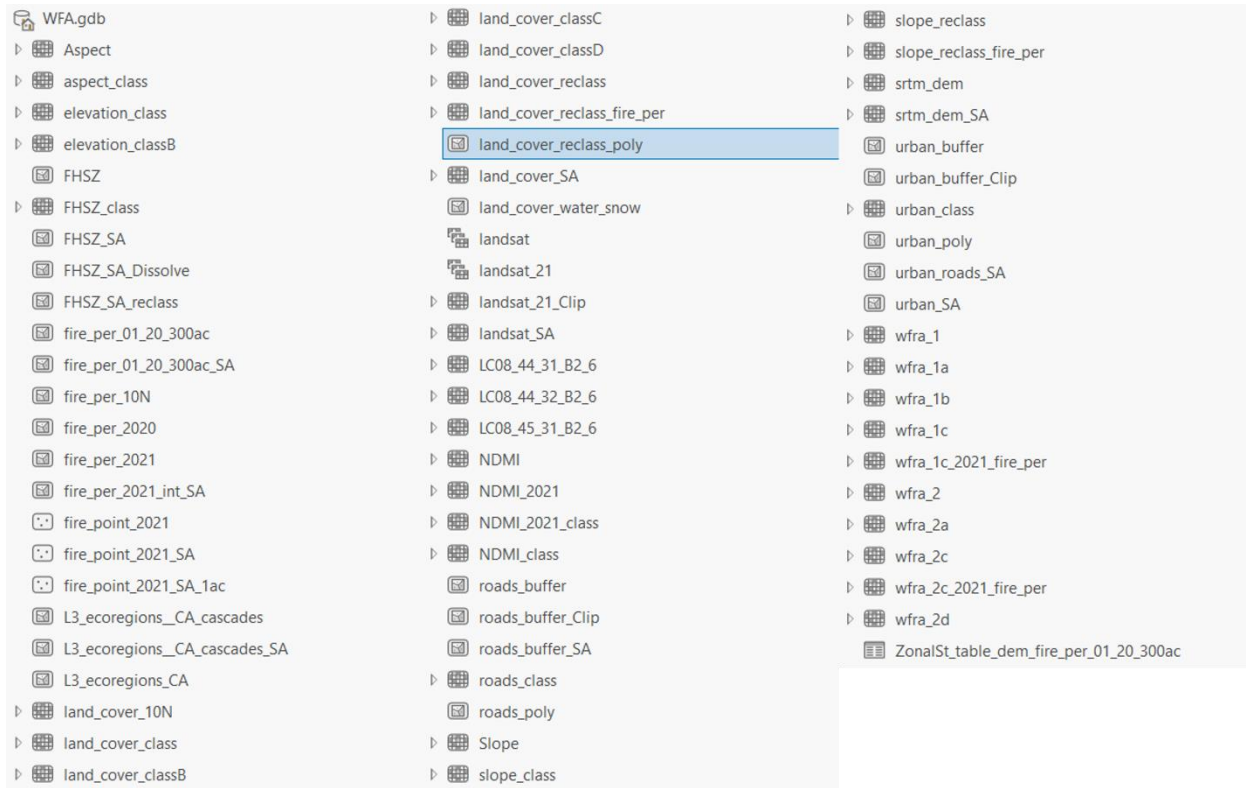


Figure A. 1 - Screenshot of working geodatabase for the WFRAs and evaluation of WFRAs.

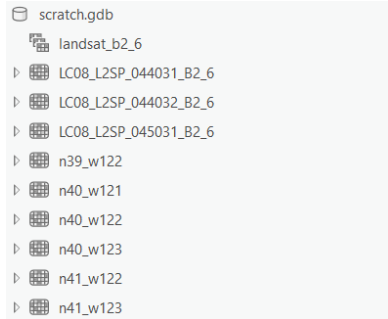


Figure A. 2 - Screenshot of scratch geodatabase for initial import Landsat and SRTM datasets.

Appendix B: Fire Risk Factors Maps

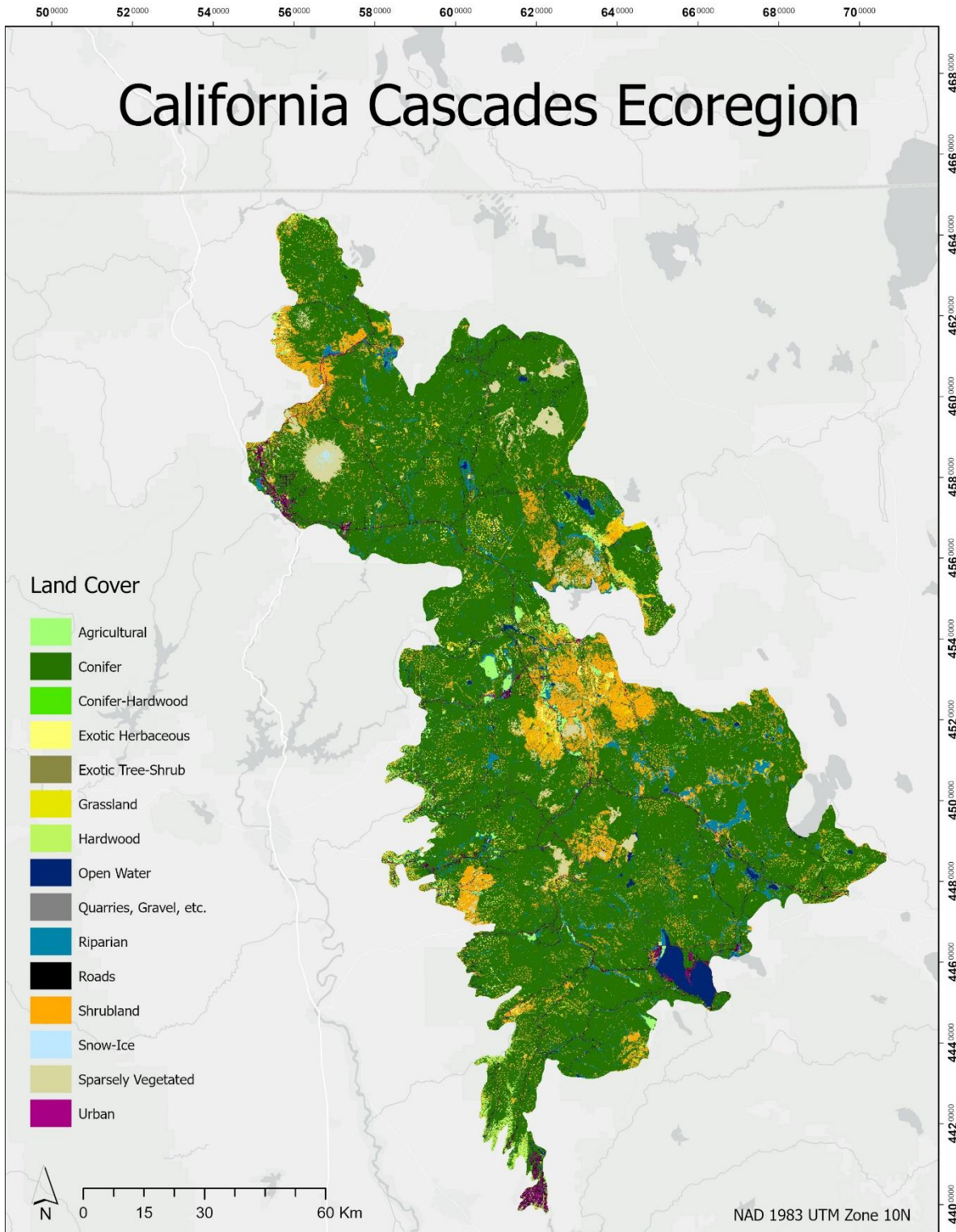


Figure B. 1 – LANDFIRE land cover classification of the study area from 2020.

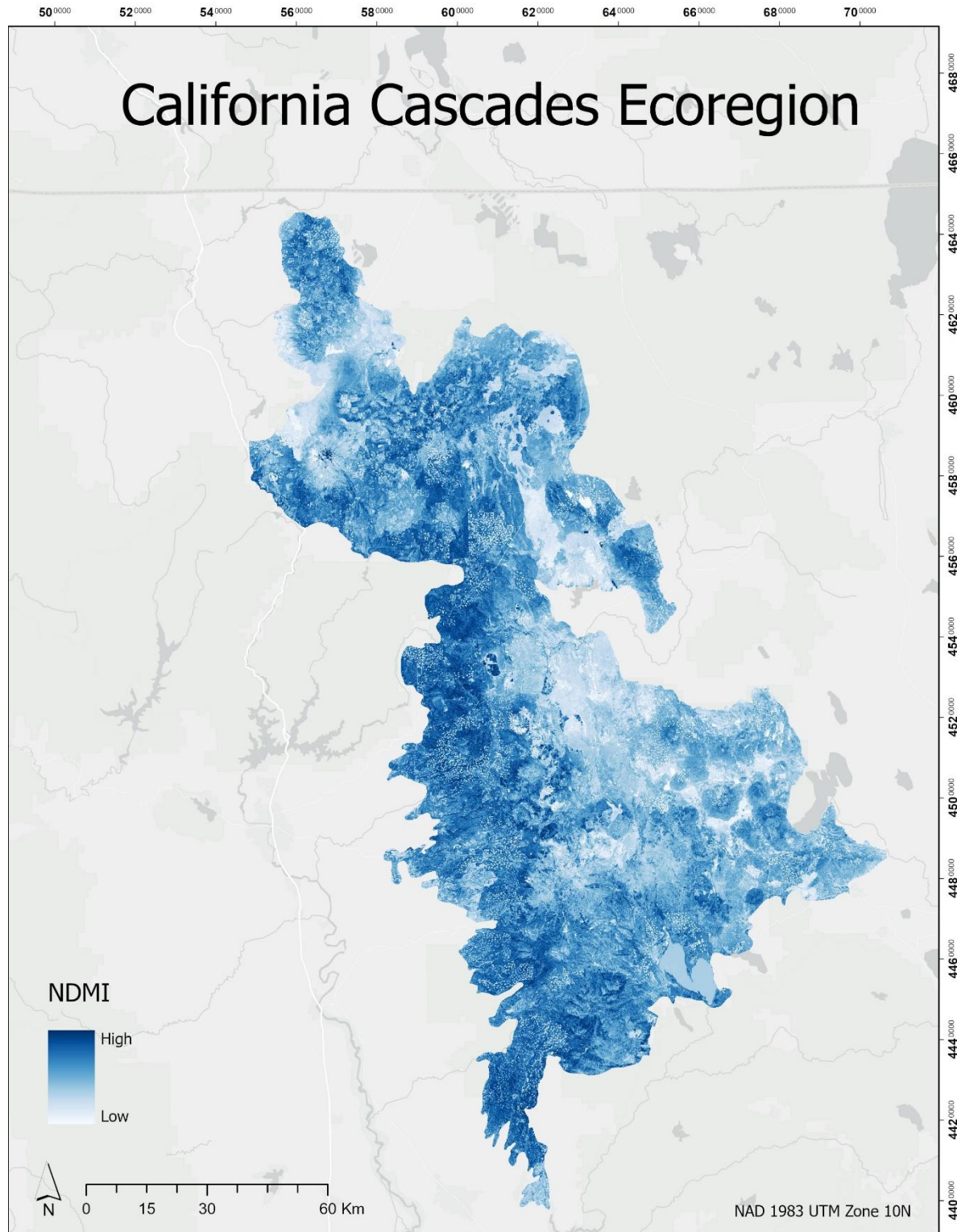


Figure B. 2 - NDMI of the study area calculated using Landsat imagery from June 25, 2021, and July 2, 2021.

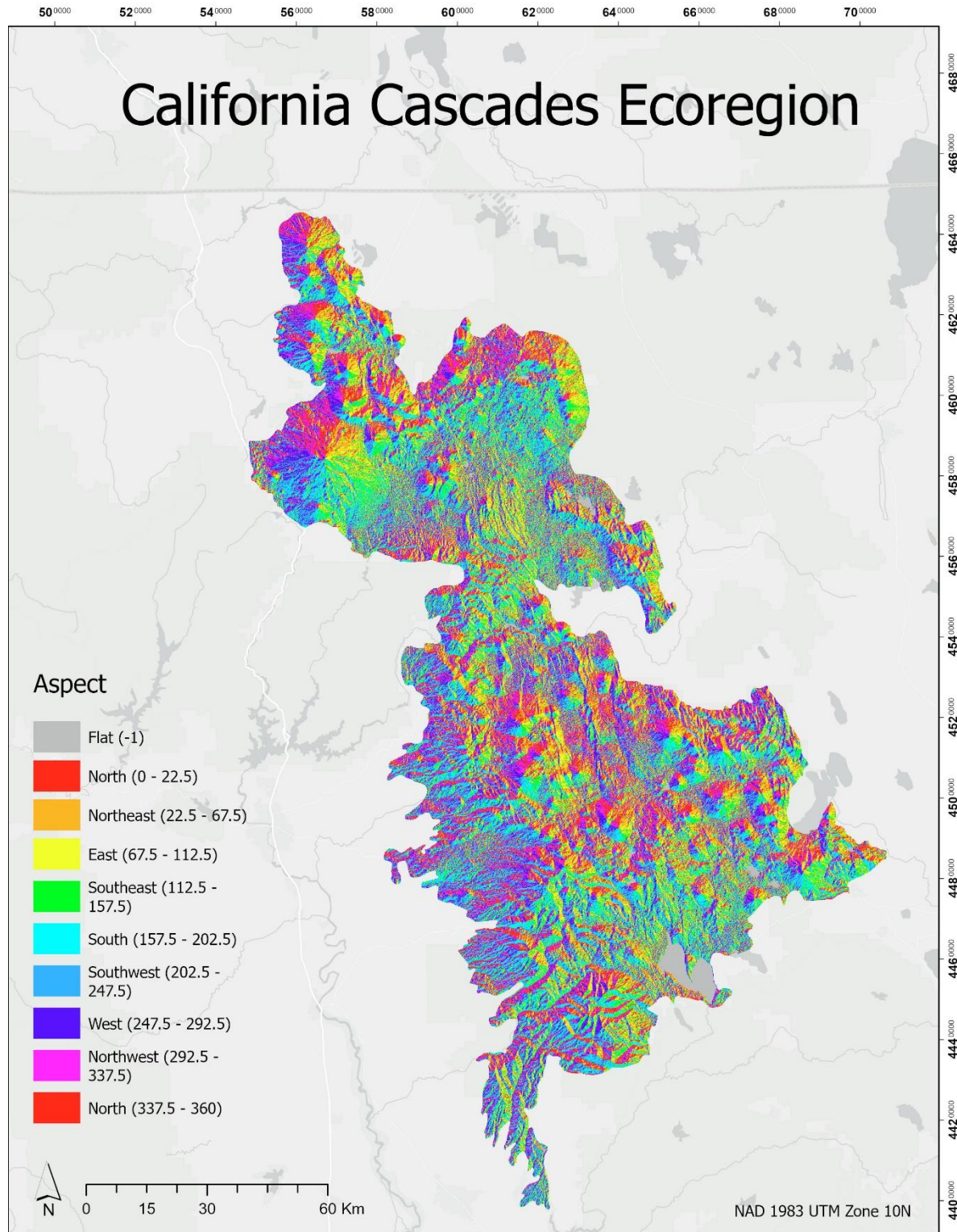


Figure B. 3 - Aspect of the study area derived from SRTM DEM.

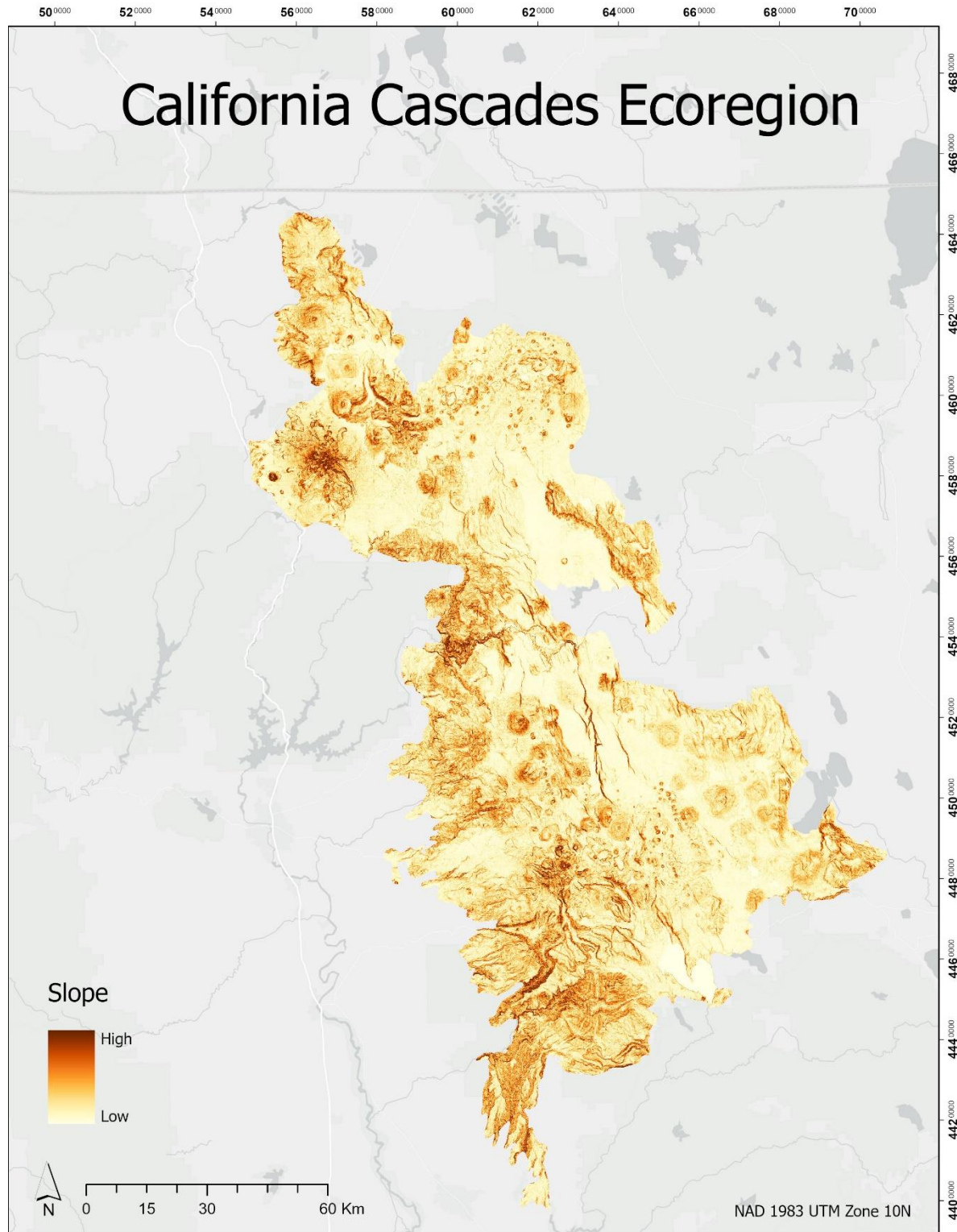


Figure B. 4 - Slope of the study area derived from SRTM DEM.

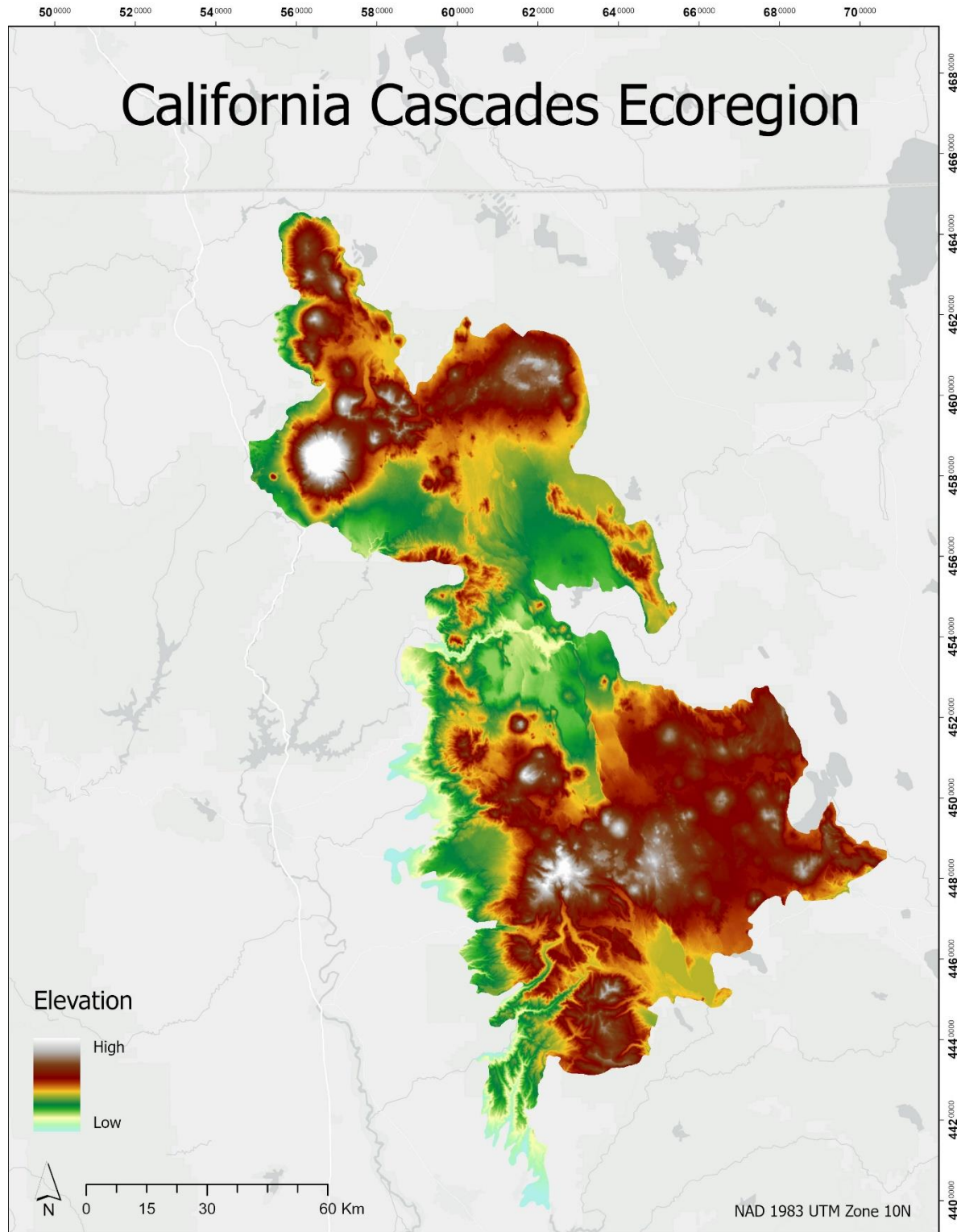


Figure B. 5 - Elevation of the study area from SRTM DEM

Appendix C: Fire Risk Factors Classification Maps

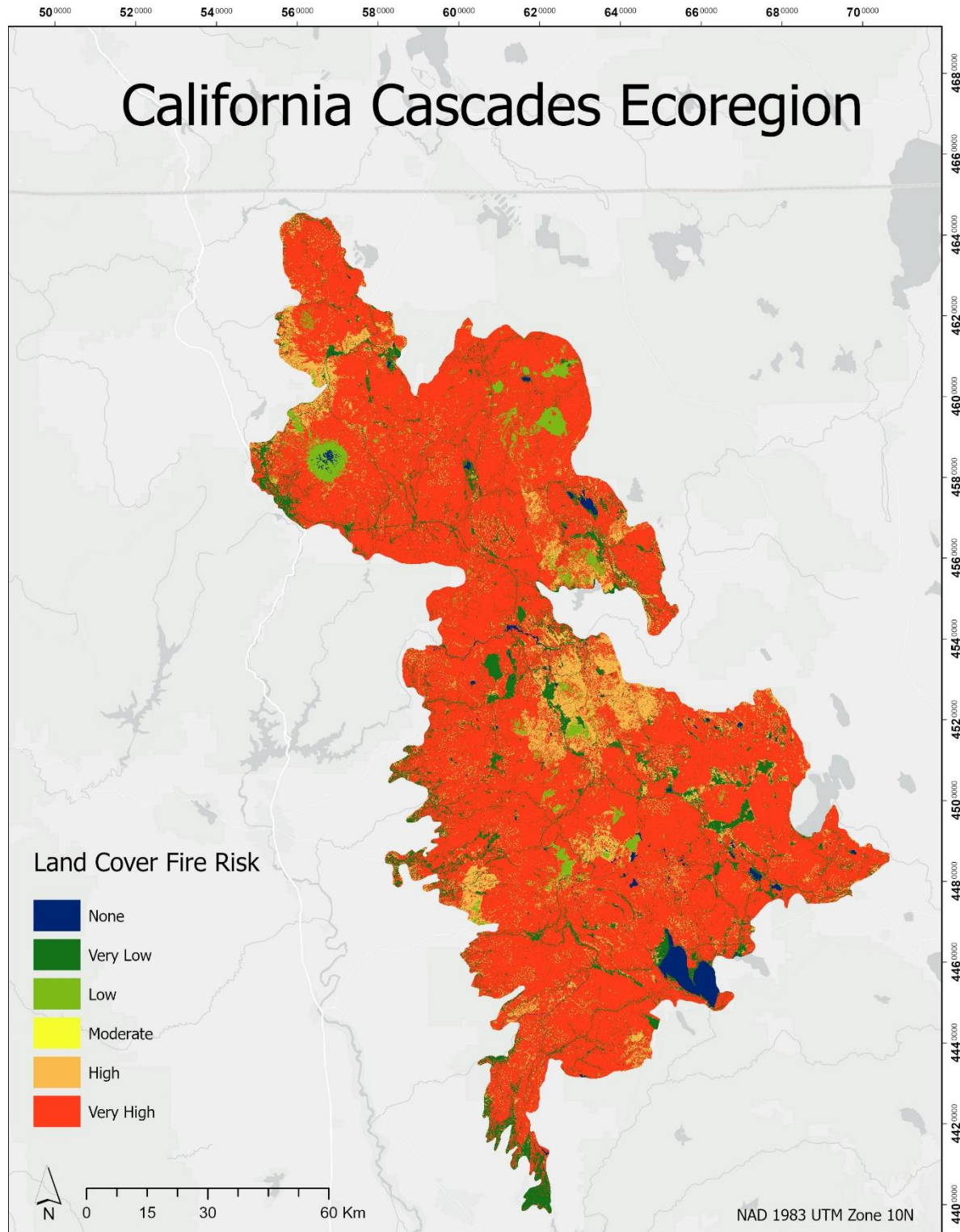


Figure C. 1 - Land cover fire risk classification.

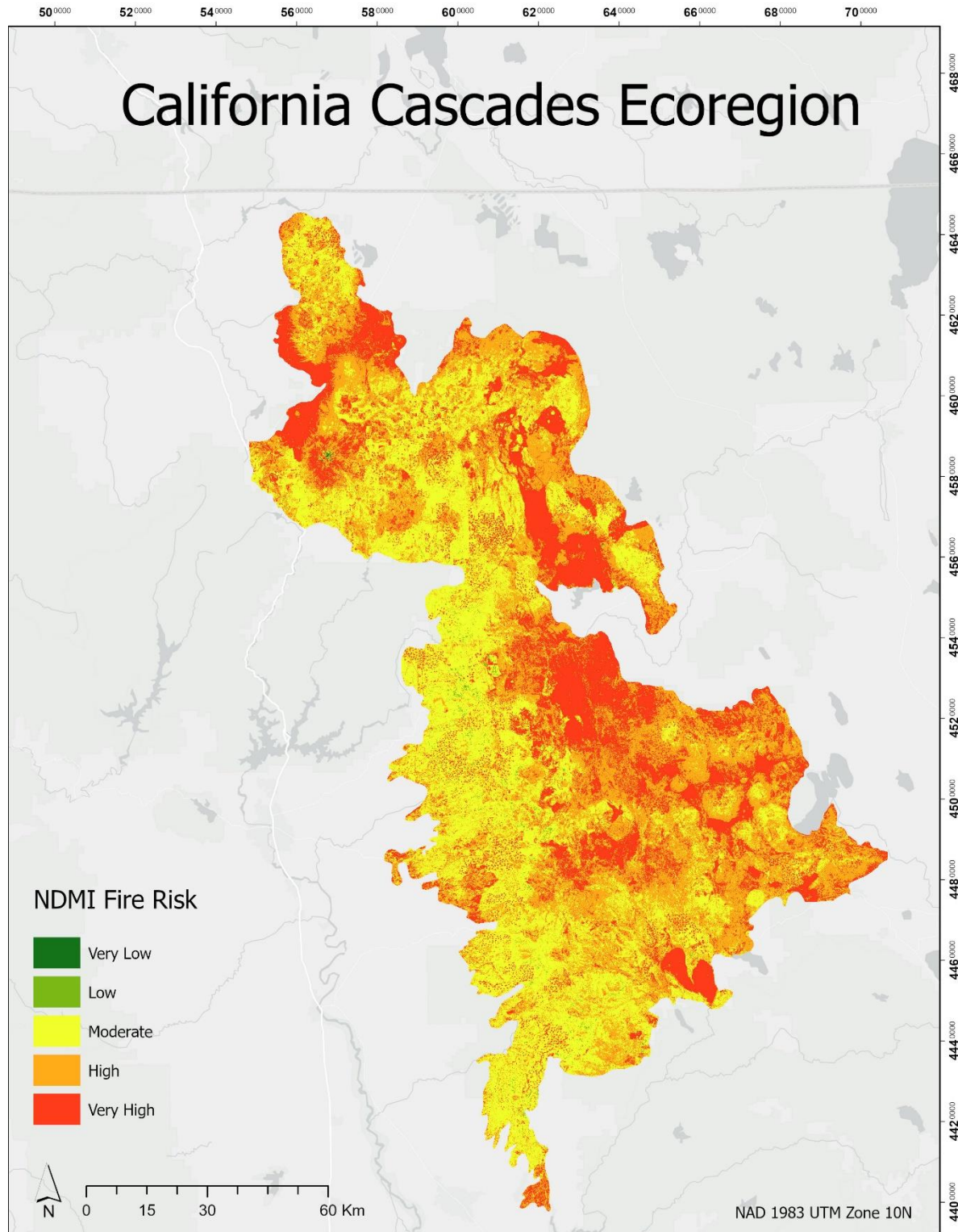


Figure C. 2 - NDMI fire risk classification.

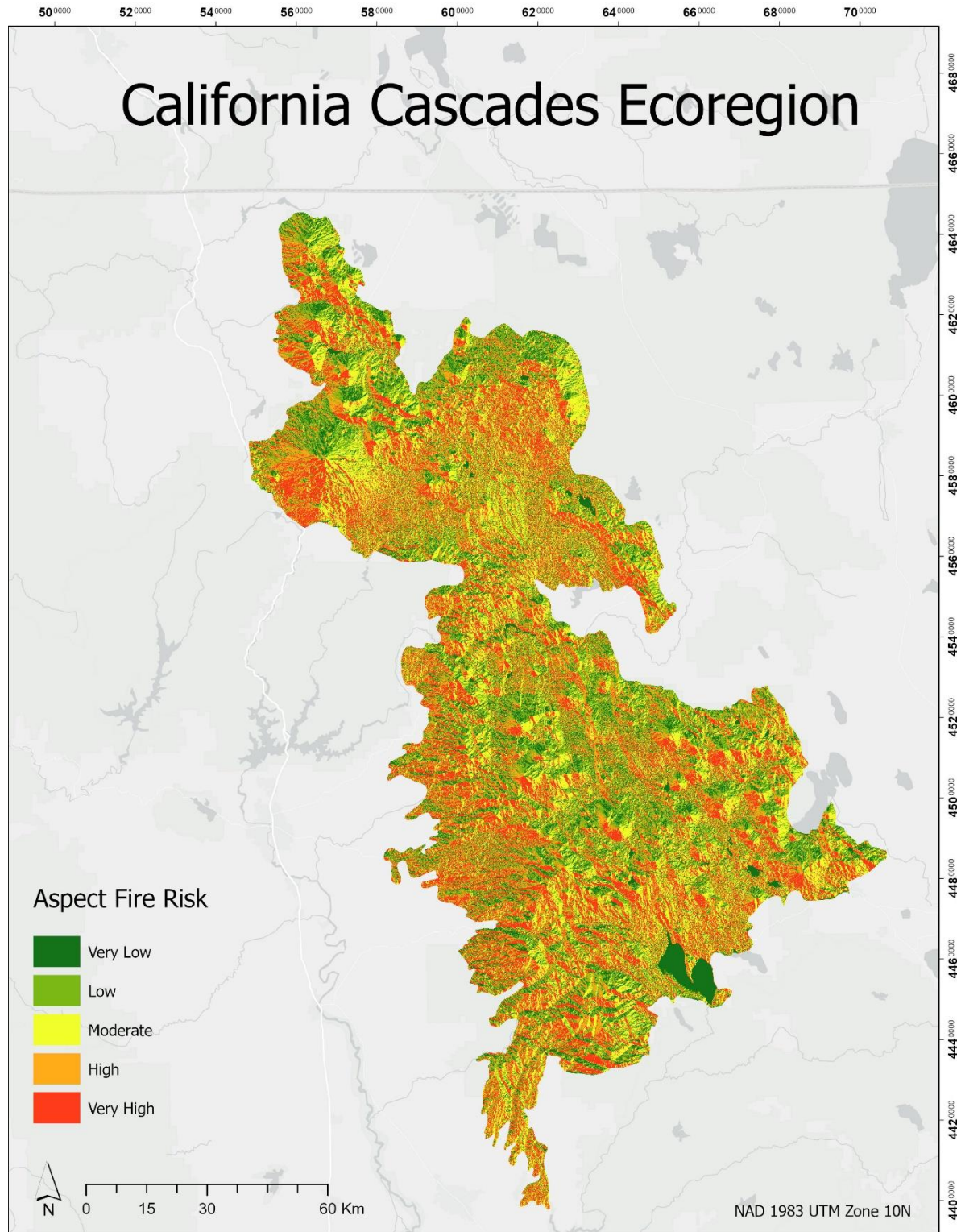


Figure C. 3 - Aspect fire risk classification.

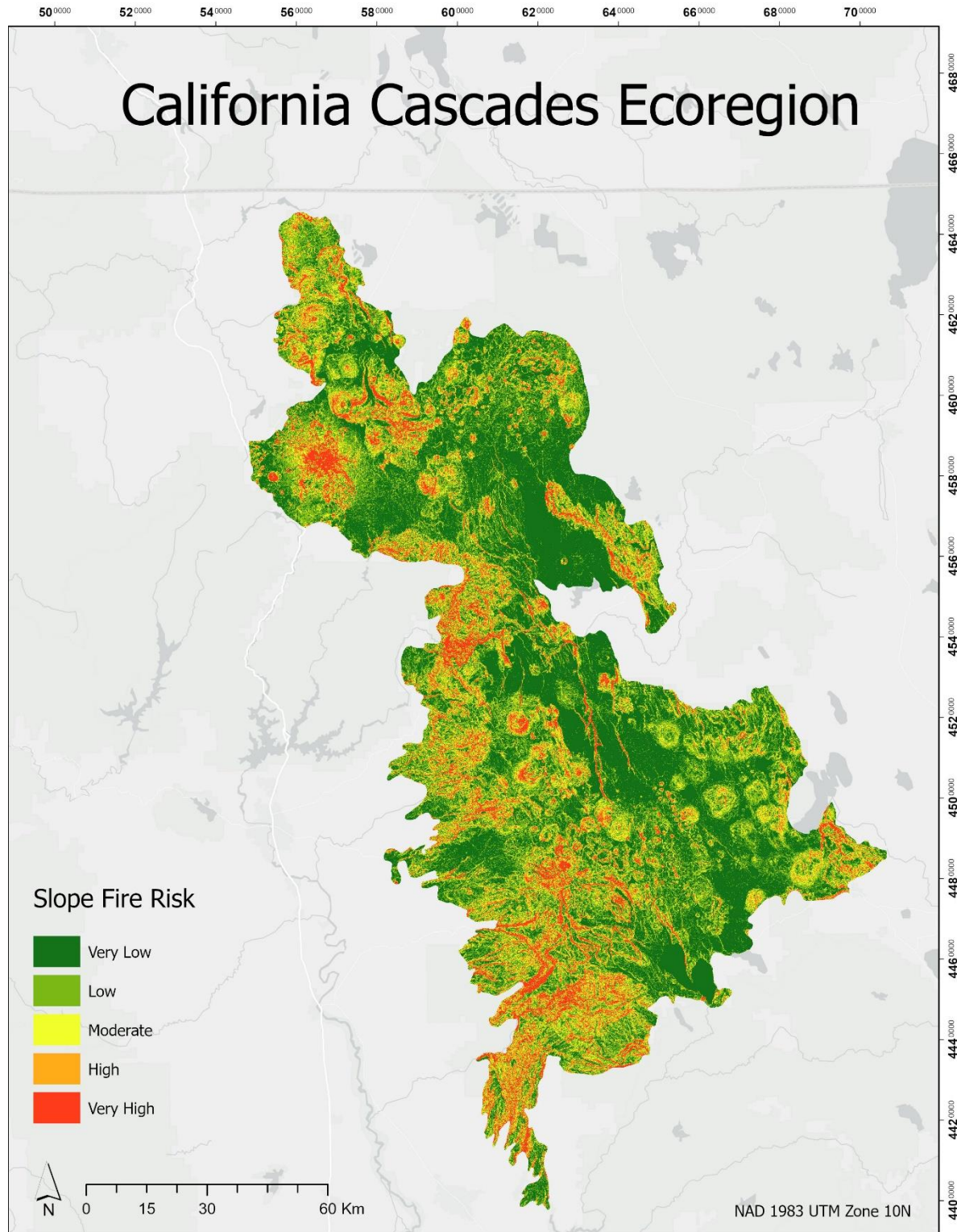


Figure C. 4 - Slope fire risk classification.

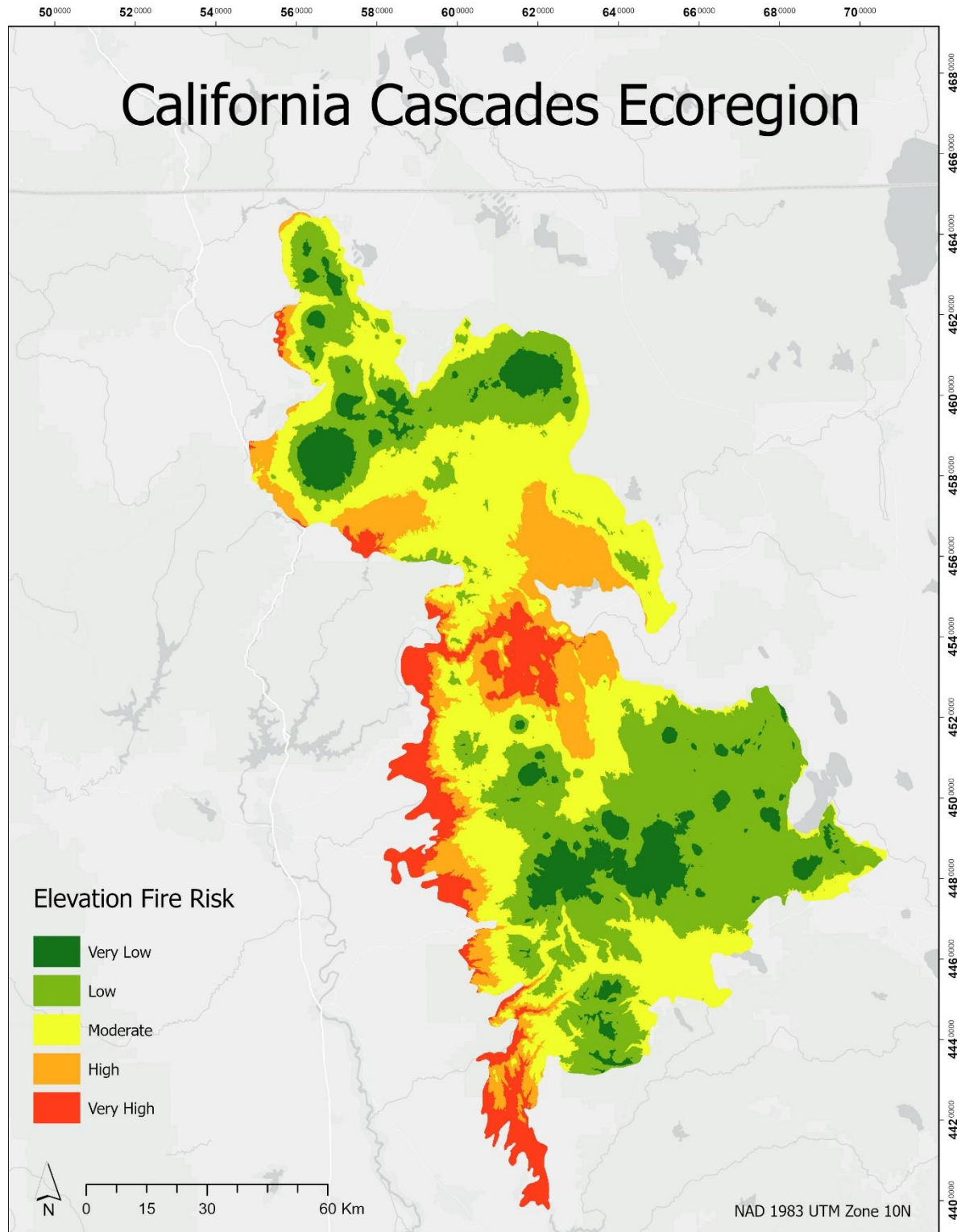


Figure C. 5 - Elevation fire risk classification.

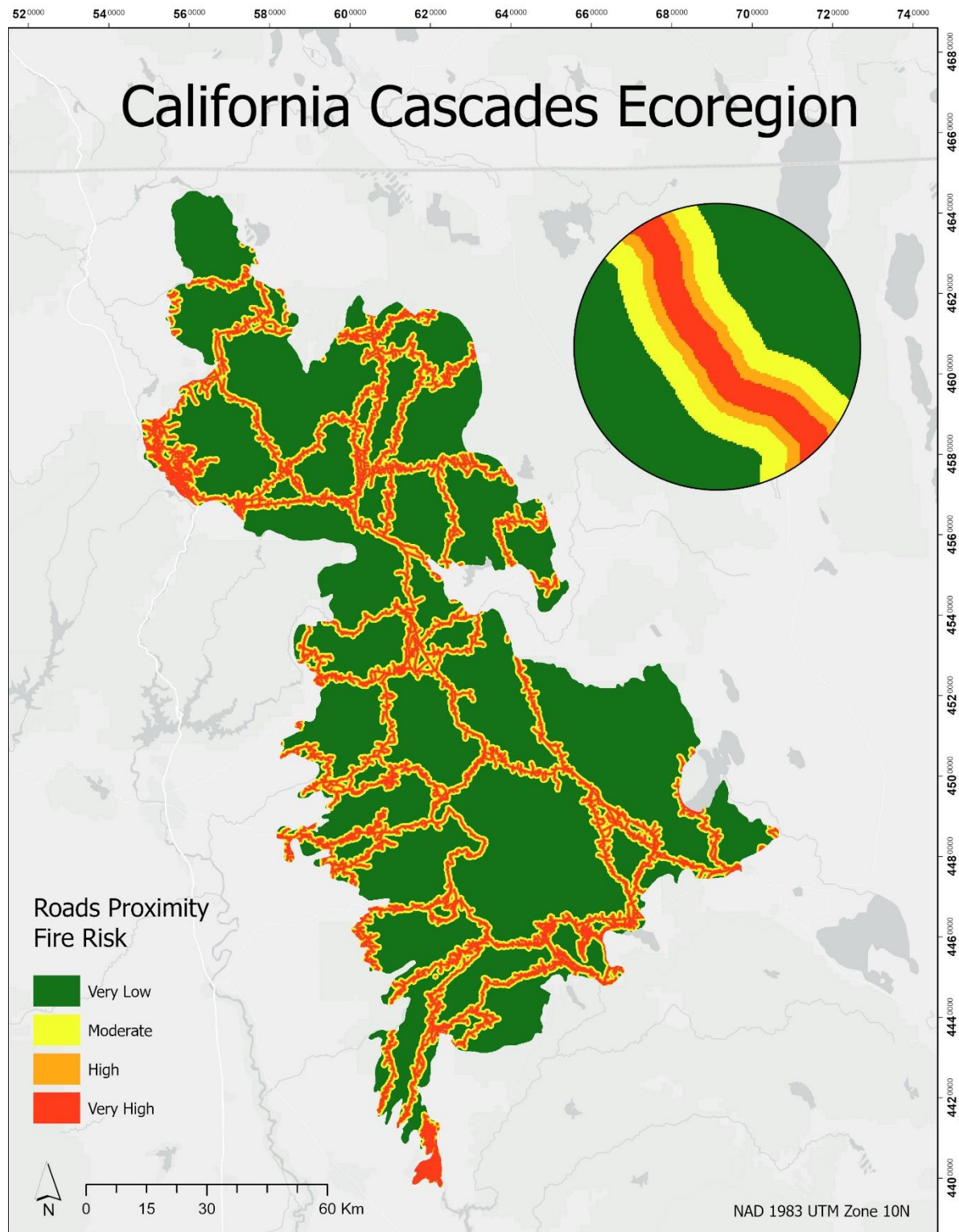


Figure C. 6 - Proximity to roads fire risk classification.

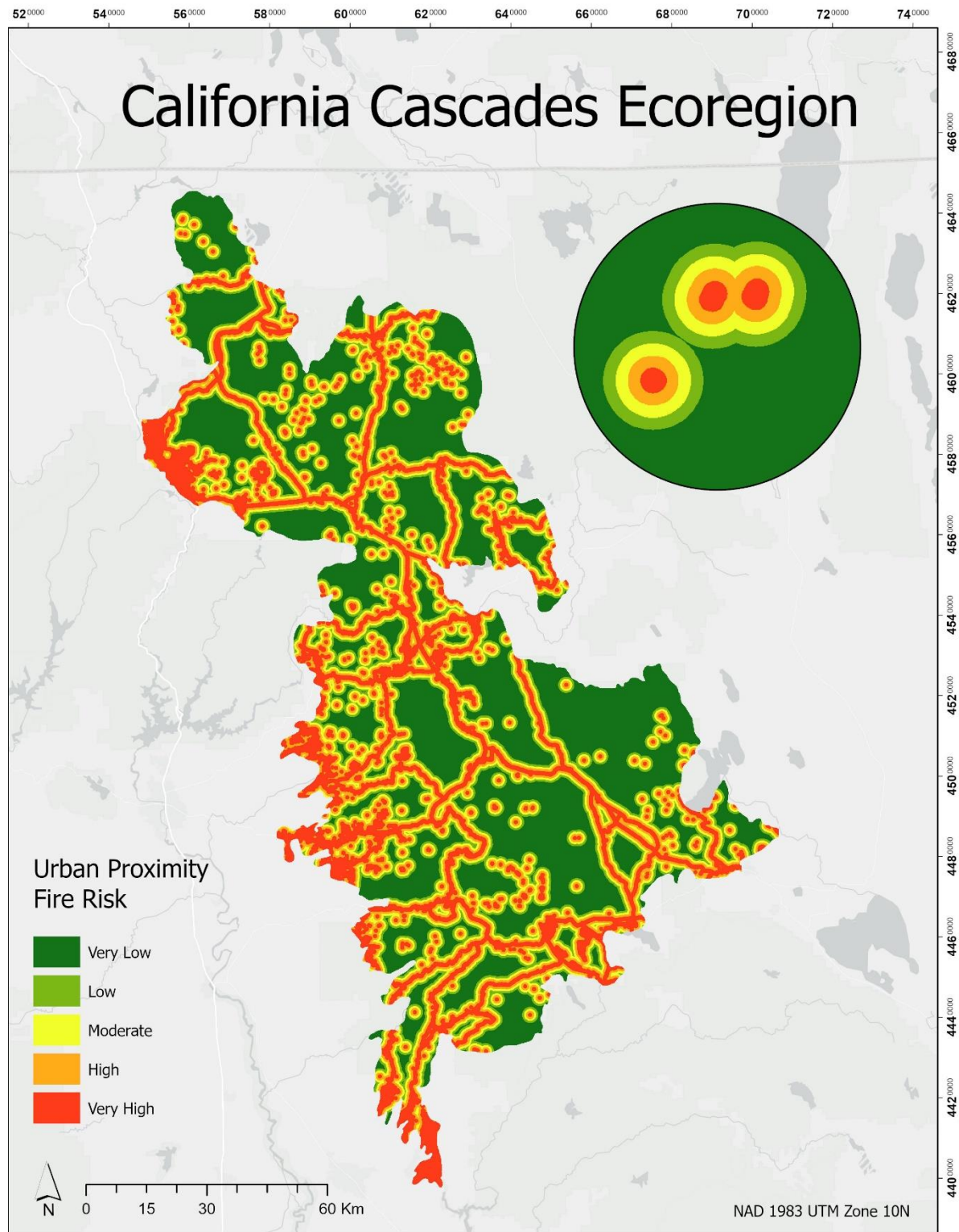


Figure C. 7 - Proximity to urban areas fire risk classification.

Appendix D: Wild Fire Risk Assessment Maps

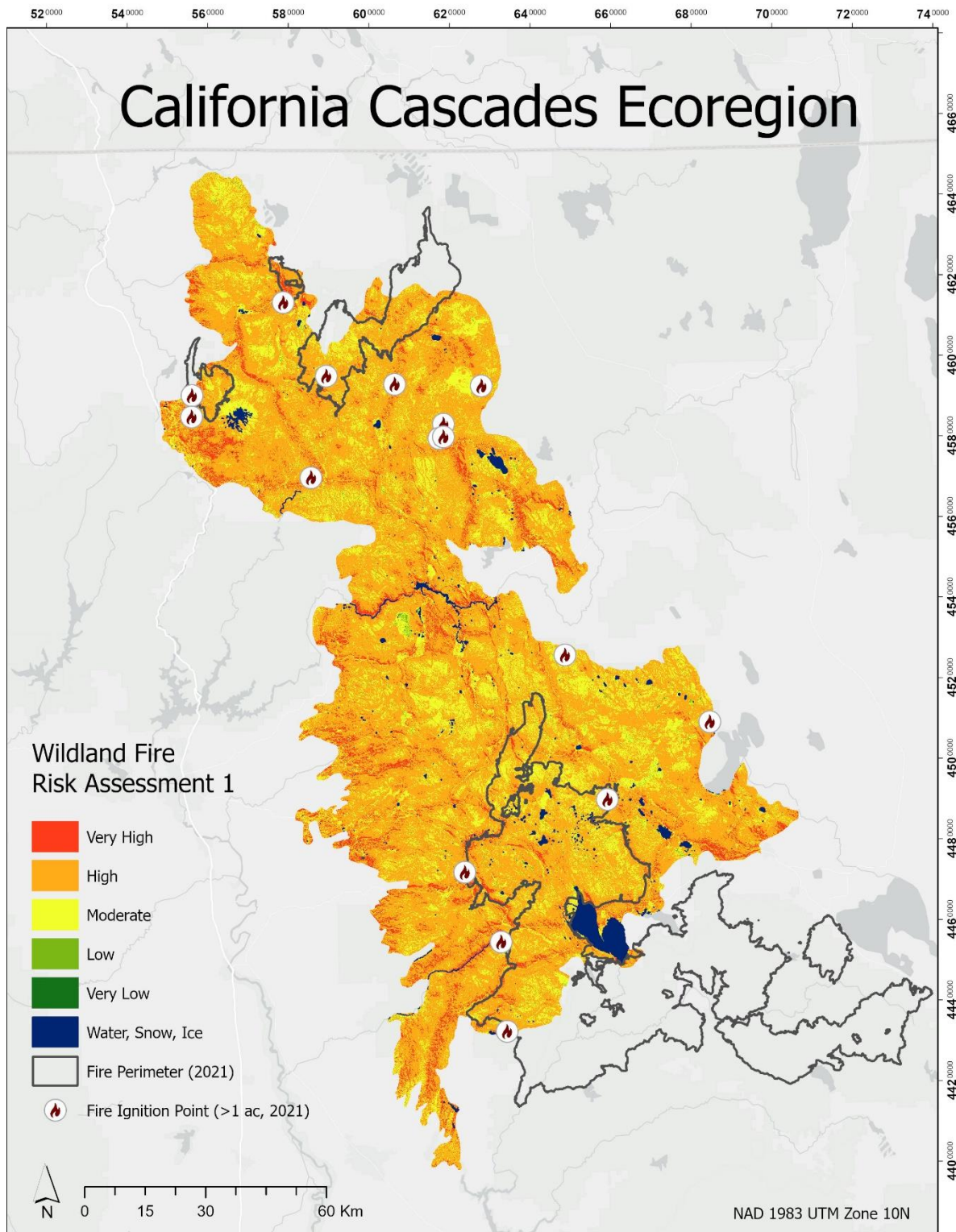


Figure D. 1 – Wildland Fire Risk Assessment 1 results.

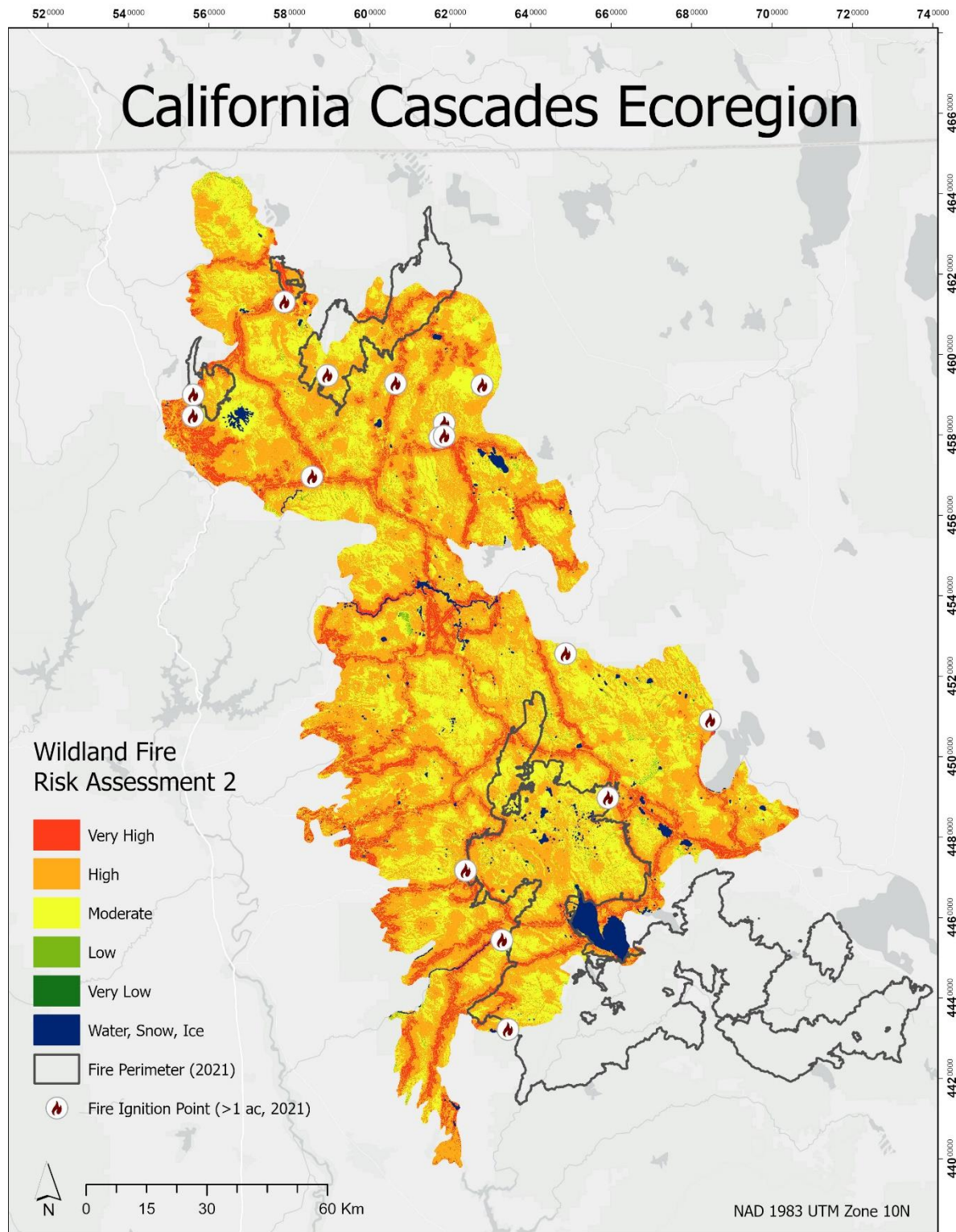


Figure D. 2 - Wildland Fire Risk Assessment 2 results.